

The effect of carborane, bicyclo[2.2.2]octane and benzene on mesogenic and dielectric properties of laterally fluorinated three-ring mesogens†

Adam Januszko,^a Kristin L. Glab,^a Piotr Kaszynski,^{*a} Kaushik Patel,^a Robert A. Lewis,^b Georg H. Mehl^b and Michael D. Wand^c

Received 4th January 2006, Accepted 18th May 2006

First published as an Advance Article on the web 20th June 2006

DOI: 10.1039/b600068a

Six series of structurally similar compounds containing 12- and 10-vertex *p*-carborane (A and B), bicyclo[2.2.2]octane (C), and benzene (D) were prepared and their mesogenic and dielectric properties investigated. Comparative analysis showed that all carborane derivatives form significantly less stable mesophases than their carbocyclic analogs, however they exhibit a relatively high shielding ability for lateral fluorination. Depression of the clearing temperature upon fluorination of series 1, 3, and 5 is approximately constant for each series A–D and correlates with the diameter of the ring \mathcal{A} (the slope = 14.8 °C Å⁻¹ and $R^2 = 0.997$). Compounds in series 2 (X = F) were used as low concentration additives to a nematic host, 6-CHBT. Dielectric parameters were extrapolated to pure additives and analyzed using the Maier–Meier equation. The Kirkwood factors g and apparent order parameters S_{app} that are required to reproduce the extrapolated dielectric values follow the trend in the size of ring \mathcal{A} . The smallest g (0.47) and the largest S_{app} (6.3) are obtained for carborane 2A, and the largest g (0.69) and the smallest S_{app} (0.7) are obtained for the terphenyl derivative 2D. The increase of S_{app} in the series D→A corresponds to the increasing disorder of the nematic solution with increasing size of ring \mathcal{A} .

Introduction

Liquid crystals with negative dielectric anisotropy ($\Delta\epsilon < 0$) are important components of materials for flat panel display applications.^{1,2} One of the most effective ways to introduce a transverse molecular dipole moment and to form materials with $\Delta\epsilon < 0$ is by using lateral fluorination of benzene rings.^{3–8} Such materials typically exhibit low viscosity and high resistivity desired for nematic and ferroelectric applications.^{2,7,9} Accumulated results also show that lateral substitution with fluorine depresses the clearing temperature of the liquid crystal compounds¹⁰ by broadening the molecular width and consequently lowering the molecular aspect ratio. The extent to which the T_{NI} is affected by such substitution depends on the size of the ring adjacent to the substitution site.¹¹

Derivatives of carboranes A and B (Fig. 1) exhibit nematogenic properties and a lower tendency for the formation of smectic phases than their isostructural analogs containing bicyclo[2.2.2]octane (C) and benzene (D) rings.^{12–15} This behavior has been ascribed to the relatively large size of the carboranes and high order rotational axes which results

in large conformational freedom of their derivatives.^{13,15,16} Recently, we demonstrated that with its large size, 12-vertex carborane A provides a particularly effective “shield” for lateral substitution as compared to the carbocyclic analogs.¹⁷ This ability of carboranes to sterically shield and promote nematogenic properties is of interest for fundamental structure–property relationship studies and in the context of developing nematic materials for electro-optical applications.

In continuation of our comparative studies of carboranes and carbocycles as structural elements for liquid crystals, we investigate here the effect of the ring structure and fluorination on the mesogenic behavior of a series of compounds 1–6 and also on the dielectric parameters of series 2 in a nematic host. The dielectric results for the binary mixtures and observed trends for extrapolated values are analysed by, and rationalized with, the aid of the Maier–Meier relationship.

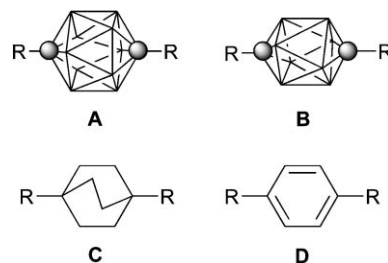


Fig. 1 Four ring systems: 1,12-dicarba-*closo*-dodecaborane (12-vertex *p*-carborane, A), 1,10-dicarba-*closo*-decaborane (10-vertex *p*-carborane, B), bicyclo[2.2.2]octane (C), and benzene (D). In A and B each vertex represents a BH fragment and each sphere is a carbon atom.

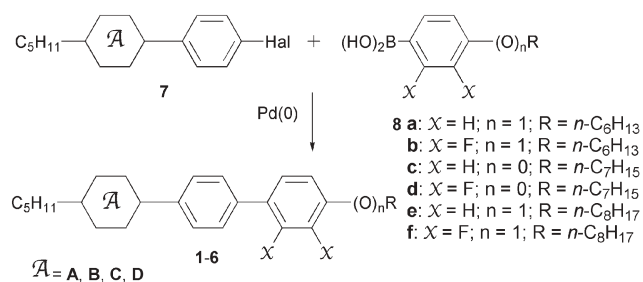
^aOrganic Materials Research Group, Department of Chemistry, Vanderbilt University, Nashville, TN, 37235.

E-mail: piotr.kaszynski@vanderbilt.edu; Fax: +1-615-343-1234; Tel: +1-615-322-3458

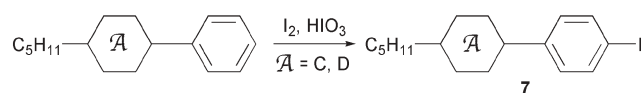
^bThe Department of Chemistry, Hull University, Hull, HU6 7RX, UK

^cLC Vision LLC, Boulder CO, 80305, USA

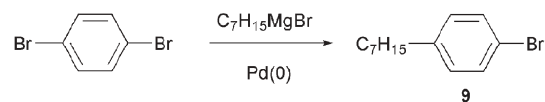
† Electronic supplementary information (ESI) available: analytical data for synthesized mesogens and their intermediates, DSC for 1D, texture photomicrographs for 3D, complete dielectric data, computational method selection, and quantum-mechanical and Maier–Meier computational details. See DOI: 10.1039/b600068a



Scheme 1



Scheme 2



Scheme 3

Results

Synthesis

Mesogens **1–6** were prepared by the coupling of aryl halide **7** and boronic acids **8** (or their esters) according to either the original¹⁸ or modified Suzuki procedures (Scheme 1). The use of a mixture of polar *N*-methylpyrrolidone (NMP) and conc. solution of K₃PO₄ in the latter reaction was found to be generally more efficient. A coupling reaction of triflate **7D** (Hal = OTf) with an ester of **8b** gave a low yield of the expected **2D**, presumably due to hydrolytic instability of the triflate in the homogenous aqueous reaction mixture. Only alkoxy derivatives in series **B** containing the 10-vertex *p*-carborane (**1B**, **2B**, **5B**, and **6B**) were prepared; the synthesis of **3B** and **4B** was not attempted due to expected significant difficulties with purification.¹⁹ Transition temperatures for three members of series **5**²⁰ and **6D**⁴ were taken from the literature.

Iodides **7C** and **7D** (Hal = I) were prepared from the corresponding hydrocarbons by iodination with I₂-HIO₃ according to a general literature procedure²¹ (Scheme 2). The bromide **7C** (Hal = Br) was prepared by a Friedel-Crafts

alkylation of bromobenzene with 1-bromo-4-pentylbicyclo[2.2.2]octane following a literature procedure.²² The preparation of bromides **7A**²³ and **7B**²⁴ was reported before.

Boronic acids **8a**,²⁵ **8b**,⁴ **8c**,²⁶ **8d**,⁴ **8e**,²⁷ and **8f**⁹ were prepared as described in the literature. 4-Bromoheptylbenzene (**9**), required for the preparation of **8c**, was conveniently obtained by Pd-catalyzed coupling of heptylmagnesium bromide and 1,4-dibromobenzene (Scheme 3), according to an analogous literature procedure.²⁸

Thermal properties

Transition temperatures and enthalpies of the mesogens were determined by differential scanning calorimetry (DSC) and the results are shown in Table 1. Phases were identified by comparison of the microscopic textures observed under polarized light with those published for reference compounds^{29–31} and based on the established order of phase stability.

Carborane derivatives **A** and **B** exhibit only a nematic phase, with the exception of **5B** and the reported²⁰ **5A** which also show a monotropic SmA. In contrast, all bicyclo[2.2.2]octane and benzene derivatives, **C** and **D**, show smectic polymorphism

Table 1 Transition temperatures (°C) and enthalpies (kJ mol⁻¹) for carborane-containing liquid crystals^a

A				
	1	2	3	6
	1: X = H; n = 1; R = <i>n</i> -C ₆ H ₁₃	2: X = F; n = 1; R = <i>n</i> -C ₆ H ₁₃	3: X = H; n = 0; R = <i>n</i> -C ₇ H ₁₅	4: X = F; n = 0; R = <i>n</i> -C ₇ H ₁₅
	5: X = H; n = 1; R = <i>n</i> -C ₆ H ₁₇	6: X = F; n = 1; R = <i>n</i> -C ₆ H ₁₇		
A	A	B	C	D
1 , X = H	Cr 103 N 160 I (27.0) (1.4)	Cr 63 N 153 I (17.7) (0.9)	Cr 100 SmB 195 SmA 221 N 227 I (18.9) (3.1) (3.8) (1.2)	Cr 95 E 207 SmB 218 SmA 230 I ^b (6.1) (5.1) (4.8) (8.7)
2 , X = F	Cr ₁ 98 Cr ₂ 99 N 132 I (6.9) (21.0) (0.9)	Cr 66 N 121 I (28.6) (0.7)	Cr 64 SmA 157 N 188 I (18.7) (1.1) (1.0)	Cr 99 SmC 145 N 165 I ^c (13.2) (1.0) (1.3)
3 , X = H	Cr ₁ 62 Cr ₂ 71 N 119 I (0.4) (25.6) (0.8)	Na	Cr 46 SmB 196 SmA 198 I (15.2) (12.7) ^d	Cr 135 ^e E 180 SmB 203.5 SmA 204.5 I (0) (5.0) (19.5) ^d
4 , X = F	Cr 90.0 N 91.5 I (33.5) (0.9)	Na	Cr 83 SmB 101 SmA 137 N 160 I (21.9) (1.0) (0.8) (0.7)	Cr 56 SmC 103 SmA 132 N 137 I ^f (21.8) (0.05) (5.2) ^d
5 , X = H	Cr 71 ⁱ (SmA 45) N 149 I ^g (20.1) (1.3)	Cr ^k 46 S _A 73 N 142 I (14.1) (0.1) (1.4)	Cr 89 SmB 190 SmA 216.4 N 217 I ^g (16.3) (2.7) (6.7) ^d	Cr 97 E 194 SmB 210.5 SmA 221.5 I ^g (12.6) (5.0) (6.7) (11.3)
6 , X = F	Cr 75 N 120 I (30.9) (0.8)	Cr 64 N 111 I (33.4) (0.6)	Cr ^j 55 SmC 77 ^e SmA 155 N 177 I (^h) (0.0) (0.8) (1.0)	Cr 93.5 SmC 144 SmA 159 I ^h

^a Cr = crystal, Sm = smectic, N = nematic, I = isotropic. ^b Lit.: Cr 205 SmB 216 SmA 228.5 I; ref. 32. ^c Lit.: Cr 97.5 SmC 145.5 N 166 I; ref. 4. ^d Sum of two phase transition enthalpies. ^e From microscopic observation—see text for details. ^f Lit.: Cr 56 SmC 105.5 SmA 131 N 136 I; ref. 4. ^g Ref. 20. ^h Ref. 4. ⁱ Cr–Cr transition at 64 °C (6.1 kJ mol⁻¹) ^j Cr–Cr transition at 48 °C (6.1 kJ mol⁻¹) and 52 °C. Combined enthalpy for the latter and melting is 13.1 kJ mol⁻¹. ^k Cr–Cr transition at 33 °C (6.3 kJ mol⁻¹)

either in combination with a nematic phase or exclusive (**3C**, **1D**, **3D**, **5D**,²⁰ and **6D**⁴). These results are consistent with literature reports for **1D**,³² **2D**,⁴ and **4D**.⁴ We found, however, a broad range E phase in addition to the reported³² SmB and SmA for **1D**. This is evident from a broad peak at 95 °C corresponding to the enthalpy of 6.1 kJ mol⁻¹, which is consistent with a typical enthalpy of 10 kJ mol⁻¹ for melting to an E phase.¹⁰ Moreover, the enthalpy of 5.1 kJ mol⁻¹ for the phase transition at 207 °C does not correspond to a usual value for Cr–SmB transition, which typically is >30 kJ mol⁻¹.¹⁰ The E phase was also found in two other terphenyl derivatives **3D** and **5D**. DSC analysis of **3D** revealed no melting peak, and only Sm–Sm and Sm–I transitions were observed. Microscopic studies of **3D** showed softening of the virgin solid crystal at about 135 °C at which temperature the sample became a viscous liquid susceptible to distortion upon mechanical stress. This fluid phase was designated as an E phase based on the characteristic texture formed upon cooling the SmB. The DSC trace for **1D** and photomicrographs of textures for **3D** are provided in the Electronic supplementary information (ESI†).

A comparative analysis of the series of compounds offered insight into the effect of structural changes on mesogenic behavior. For better visualization, the series was grouped according to structural features, and clearing temperatures for derivatives **A**, **B** and **C** relative to those of the benzene analogs **D** are plotted in Fig. 2. Analysis showed that for the non-fluorinated derivatives (**1**, **3**, **5**) the order of the mesophase stability follows **D** > **C** > **A** > **B**, while in the fluorinated series (**2**, **4**, **6**) the BCO derivatives exhibit the highest clearing temperatures. In the first group of compounds, clearing temperatures of BCO derivatives are close to those of benzene analogues **D** with an average $\Delta T_{MI} = -5$ °C, while the largest difference in T_{MI} of about -79 °C is observed for the 10-vertex carborane derivatives **B**. The difference between T_{MI} for 12-vertex and benzene derivatives is almost constant for the alkoxy derivatives, but it increases significantly for the alkyl derivatives **3** and **4**. Thus, the graph reflects differences in the effect of fluorination and O→CH₂ substitution on mesogenic behaviour between each series **A–D**.

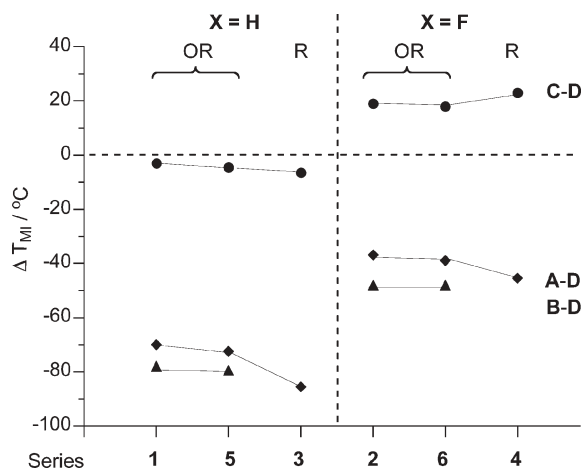


Fig. 2 Clearing temperatures for 12-vertex *p*-carborane (**A**, ◆), 10-vertex *p*-carborane (**B**, ▲), and bicyclo[2.2.2]octane (**C**, ●) derivatives relative to the T_{MI} for the benzene derivatives **D**. The lines are guides for the eye.

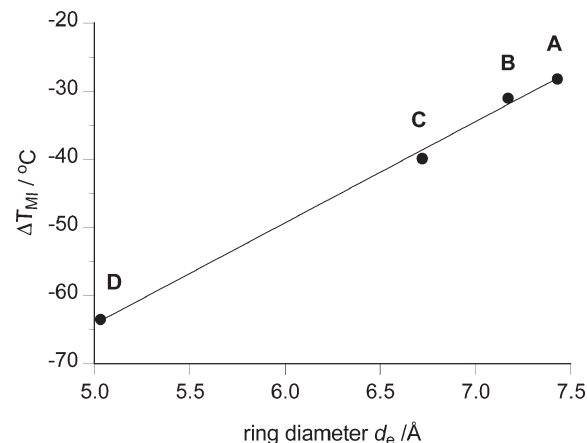


Fig. 3 Average change in clearing temperatures (ΔT_{MI}) upon fluorination in series **1**, **3**, and **5** plotted as a function of effective VDW diameter of the ring \bar{A} . Best fit line $\Delta T_{MI} = 14.8 \times d_e - 138.4$ ($R^2 = 0.997$).

Fluorination generally decreases the clearing temperatures for all series and the trend in the ΔT_{MI} follows the order in the series **A**→**D** (Fig. 3). The smallest destabilization of the mesophase by about 28 °C is observed for the carborane pairs **1A–2A**, **3A–4A**, and **5A–6A**, while for the benzene analogues the average destabilization of T_{MI} is 64 °C. The ΔT_{MI} values for the three pairs are within 1 °C in series **A**, **B**, and **C**, while in series **D** the values differ by as much as 7 °C. The observed trend in the ΔT_{MI} parallels the decrease of effective van der Waals ring size³³ d_e of the ring \bar{A} from the largest for carborane ring (**A**) to the smallest for benzene (**D**).

Other phase transitions in series **2** are also affected by introduction of the fluorine atoms. A comparison of data for the Sm–N or SmA–I transitions shows that fluorination depresses smectic phases in the hydrocarbons by about 62 °C for **C** and by an average of 73 °C for benzene derivatives **D**. It also induces a SmC phase in benzene derivatives **D** and also in **5C**. Melting points of the alkoxy derivatives **A** and **D** are little affected by fluorination. In contrast, introduction of fluorine to derivatives **1C** and **5C** decreases their melting points by about 35 °C while **5B** melts 18 °C lower than **6B**. Heptyl derivatives **3** are more strongly affected by fluorination. The melting points of the 12-vertex carborane **3A** and BCO **3C** are increased by fluorination, while the melting point of **3D** is depressed by almost 80 °C in the fluoro derivative **4D**.

Replacement of the oxygen linking the alkyl chain and the core in **1** and **2** with a CH₂ group in **3** and **4** results in significant depression of the clearing temperatures (Fig. 4). For the hydrocarbon series **C** and **D** this destabilization is about 30 °C, while for the carborane **A** the T_{NI} is lower by 41 °C. This is consistent with our other observations of generally larger stabilization of the nematic phase upon CH₂→O replacement in carborane mesogens than in the benzene analogs.³⁴

Dielectric measurements

To assess the effect of ring \bar{A} on electro-optical properties, compounds in series **2** were investigated as low concentration

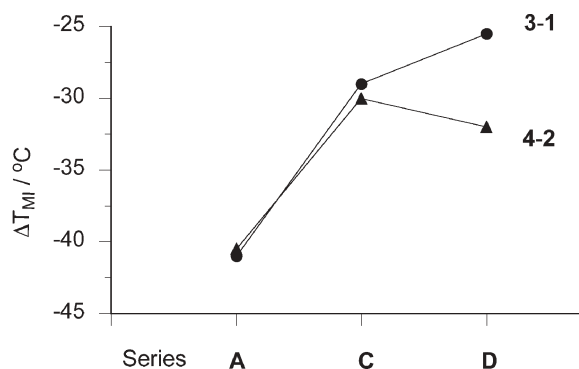


Fig. 4 Effect of O \rightarrow CH₂ change on the clearing temperature T_{MI} for fluorinated (▲) and non-fluorinated (●) series. The lines are guides for the eye.

additives to a nematic host with positive dielectric anisotropy ($\Delta\epsilon > 0$). On the basis of our previous experience³⁵ we selected 6-CHBT as a suitable host, and dielectric constants were measured for solutions of each compound **2** in three concentrations ranging from about 4 mol% to 17 mol%.

Dielectric constants for each compound **2** were obtained by linear extrapolation of the data for the solutions and the pure host. To lower the error for the extrapolated values, the intercept in the fitting function was set at the appropriate value for the pure host. A sample of data analysis is presented for **2A** in Fig. 5, and all results are collected in Table 2. Results show that the extrapolated transverse dielectric permittivity ϵ_{\perp} is similar for all compounds in series **2** and falls in a narrow range of 6.4–6.8. In contrast, the longitudinal values vary substantially from $\epsilon_{\parallel} = 4.7$ for **2D** to $\epsilon_{\parallel} = 1.1$ for **2A**, which results in marked differences in $\Delta\epsilon$ in the series.

The quality of the data fit to linear functions was excellent for **2A** and **2C** and the resulting error on the extrapolated values was <0.3 units. For **2D** a noticeable non-linear behaviour was observed for a concentration of 15 mol%, and the highest concentration used for the extrapolation was about

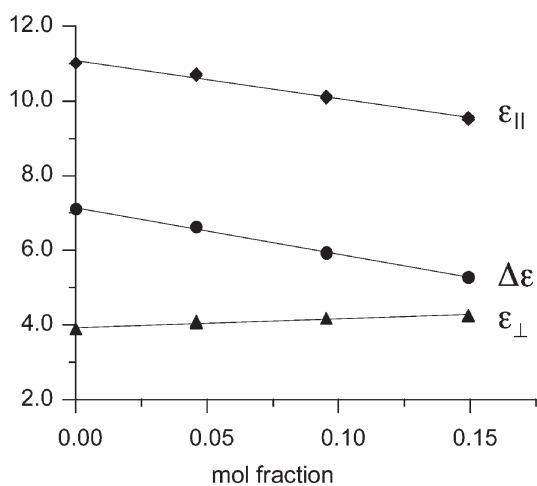


Fig. 5 Plot of ϵ_{\parallel} (◆), ϵ_{\perp} (▲), and $\Delta\epsilon$ (●) vs. concentration x of **2A** in 6-CHBT. Datapoints were fitted to functions $y = 11.0 + x\epsilon_{\parallel}$, $y = 7.1 + x\Delta\epsilon$, $y = 3.9 + x\epsilon_{\perp}$. Correlation parameters $R^2 > 0.99$ for ϵ_{\parallel} and $\Delta\epsilon$, and $R^2 = 0.98$ for ϵ_{\perp} .

Table 2 Dielectric parameters for **2** extrapolated from 6-CHBT solutions at 25 °C^a

	A	B	C	D
ϵ_{\parallel}	1.1 \pm 0.1	2.5 \pm 0.5	4.2 \pm 0.25	4.7 \pm 0.8
ϵ_{\perp}	6.4 \pm 0.2	6.8 \pm 0.3	6.5 \pm 0.3	6.8 \pm 0.3
$\Delta\epsilon$	-5.3 \pm 0.2	-4.3 \pm 0.7	-2.3 \pm 0.2	-2.1 \pm 0.55

^a Full experimental details in ESI.

10 mol%. The observed deviation from linear behaviour and consequently the higher error for extrapolated values of **2B** in 6-CHBT parallels other observations for binary mixtures involving 10-vertex mesogens.^{13,36} Each individual datapoint for binary mixtures used for the extrapolation represents an average of 10 repetitive measurements in a single cell and has an associated error of <0.02 units. Since cell parameters vary slightly, reproducibility of the measurement from cell to cell is lower and a typical error for a multi-cell analysis is about 0.08 units. Thus, dielectric parameters for the host have an error of 0.08 established by averaging results for three cells. This relatively high uncertainty for the measured values is partially eliminated in the fitting process of three datapoints from three different cells.

Computation of molecular parameters

To rationalize the observed trends in the extrapolated dielectric properties, dipole moments μ and electronic polarizabilities α were calculated for **2** at standard orientation using the HF the B3LYP methods respectively.³⁷ Reorientation of the molecules from Gaussian standard orientation (nuclear charge based) to the principal moment of inertia coordinates (mass based) had a negligible effect on the angle β ($+0.3^\circ$) between μ and μ_{\parallel} . Results in Table 3 show that the transverse dipole moment μ_{\perp} is the dominant (about 3.8 D) and virtually invariant for all compounds in the series. It originates from the two polar C–F bonds reinforced by the C–O bond of the coplanar alkoxy substituent whose alkyl chain is oriented *anti* to the fluorine atoms. In contrast, the longitudinal dipole moment μ_{\parallel} varies significantly in the series. It reflects the electron withdrawing ability of the ring **A** and correlates well with the ring ρ_p parameters:³⁸ **A** (0.14)³⁹ **B** (0.05)³⁹ **C** (-0.13),⁴⁰ and **D** (4-EtPh, -0.02).⁴¹ The two dipole moment components μ_{\perp} and μ_{\parallel} define the orientation of the net molecular dipole moment vector which is approximately orthogonal to the long molecular axis. The smallest angle β of 73° is calculated for the 12-vertex carborane derivative with the largest longitudinal dipole moment component, and the vector closest to orthogonality is found for the BCO derivative with the smallest μ_{\parallel} .

The calculated average polarizability α_{avg} decreases from the most polarizable 12-vertex carborane to the terphenyl

Table 3 Calculated molecular parameters for **2**^a

\bar{A}	A	B	C	D
μ_{\parallel}/D	1.14	0.90	0.51	0.71
μ_{\perp}/D	3.63	3.76	3.84	3.78
μ/D	3.80	3.86	3.88	3.85
β°	73	77	82	79
$\Delta\alpha/\text{\AA}^3$	50.4	52.0	43.9	53.1
$\alpha_{\text{avg}}/\text{\AA}^3$	57.1	55.1	49.4	48.7

^a Dipole moments obtained with the HF/6-31G(d) method and electronic polarizabilities at the B3LYP/3-21G level of theory. ^b The dipole moment vector is orientated from \bar{A} (negative) to OC_6H_{13} (positive). ^c Angle between the net dipole vector μ and long molecular axes calculated from the vector components. For details see ESI.

derivative (**2A** > **2B** > **2C** > **2D**). In contrast, the terphenyl derivative **2D** has the largest anisotropy of polarizability $\Delta\alpha$, and the carboranes exhibit intermediate values of $\Delta\alpha$ in the series (**2D** > **2B** > **2A** > **2C**). The observed trends are consistent with our findings for another series of mesogens³⁵ and are related to the electronic structure of the two carborane cages. Both of the carboranes **A** and **B** have highly polarizable sigma-delocalized electrons, which results in high average electronic polarizability. Due to their ellipsoidal distribution, however, anisotropy of polarizability is small.⁴²

Dielectric data analysis. The experimental values for the extrapolated transverse dielectric permittivity ϵ_{\perp} are approximately constant, which is consistent with a narrow range of μ_{\perp} values calculated for series **2** (Table 3). In contrast, the longitudinal component of the dipole moment varies significantly in the series from the lowest for the BCO derivative **2C** ($\mu_{\parallel} = 0.51$ D) to the highest for the carborane **2A** ($\mu_{\parallel} = 1.14$ D). A comparison of μ_{\parallel} values with the experimental dielectric results for **2** (Table 2) shows that the increasing dipole corresponds to decreasing ϵ_{\parallel} values. This is contrary to the expectations based on the general relationship between these two parameters ($\epsilon_{\parallel} \sim (\mu_{\parallel})^2$). To shed more light on this unexpected result, dielectric data were analyzed quantitatively using the Maier–Meier equation,⁴³ which relates the dielectric anisotropy of the nematic phase and molecular parameters (eqn 1).⁴⁴ Using this equation, dielectric behaviour of compounds **2** was evaluated in solution with 6-CHBT and also in the pure state.

$$\Delta\epsilon = \frac{NFh}{\epsilon_0} \left\{ \Delta\alpha - \frac{F\mu_{\text{eff}}^2}{2k_{\text{B}}T} (1 - 3\cos^2\beta) \right\} S \quad (1)$$

For calculations involving binary mixtures, the medium was assumed to be the pure host, and the effect of the additive was ignored. Therefore, the reaction field factor F and the cavity factor h in eqn 1 were calculated for pure 6-CHBT using experimental optical and dielectric data.⁴⁵ With this

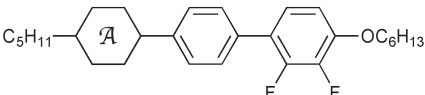
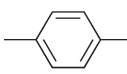
assumption, apparent order parameters, S_{app} , were obtained from the extrapolated dielectric anisotropy $\Delta\epsilon$ by systematically varying the Kirkwood factor⁴⁶ g in such a way that the reverse calculations reproduce the extrapolated dielectric parameters ϵ_{\parallel} and ϵ_{\perp} for each compound. The factor g relates μ^2 and μ_{eff}^2 and is the only adjustable quantity in eqn 1. Varying the angle β had little effect on ϵ_{\parallel} , which appears to be the most critical of the two dielectric components. The resulting g and S_{app} values are listed in Table 4, and details of calculations are described in the ESI†.

Analysis of results in Table 4 shows that both experimental dielectric components, ϵ_{\parallel} and ϵ_{\perp} , are very closely reproduced by calculations. This is remarkable considering that dielectric anisotropy $\Delta\epsilon$ was the only experimental input value for the dopants. The Kirkwood factor g necessary to reproduce the experimental permittivities follows the trend in the ring size and varies from the smallest, 0.47, for the carborane **2A**, to the highest, 0.69, for **2D**. The observed range of g is typical for nematogens such as 6-CHBT and 5CB.⁴⁷ The most surprising result of this analysis, however, is that the apparent order parameter S_{app} is required to be greater than unity(!).

To verify the correctness of the calculations, dielectric properties of **2** in 6-CHBT were estimated using arbitrarily chosen S and g values. Thus, for assumed parameters $S = 0.7$ and $g = 1.0$, values typically used in analogous calculations,^{48,49} all calculated dielectric parameters fall in relatively narrow ranges, and $\Delta\epsilon$ increases in the series from **2A** to **2C** (Table 4). This order of $\Delta\epsilon$ values is in agreement with the expectations and results from the decreasing magnitude of the longitudinal dipole moment in the series. Also the estimated $\Delta\epsilon$ for **2C** is consistent with extrapolated values for similar compounds.^{2,3,5} These estimated dielectric values for **2** are, however, significantly different from those extrapolated from 6-CHBT solutions. Thus, not only is the calculated range too narrow, but also the trend is opposite relative to the experimentally observed $\Delta\epsilon$ values (Table 2), if normal behaviour of all additives **2** in solution is assumed. Similar dielectric values and trends were predicted for pure mesogens **2** (Table 2), which are consistent with other computational results.⁴⁸

Analysis of the dielectric results clearly shows that the extrapolated highly negative $\Delta\epsilon$ requires a small ϵ_{\parallel} which can be calculated only by allowing physically unrealistic S_{app} values. So what does the apparent order parameter S_{app} mean, and what is the physical significance of $S_{\text{app}} > 1$? The Maier–Meier equation (eqn 1) can be presented in a simplified form in which $\Delta\epsilon$ is the product of the molecular parameter C and order parameter S . Consequently, ideal additivity of $\Delta\epsilon$ for a binary mixture can be expressed as eqn 2, in which x represents mole fraction and S_i is the individual order parameter. Since the original extrapolation ignored the effect of the additive **2** on properties of the host (including the order parameter), S_{app} represent a factor which corrects for this assumption. Consequently, a large value for S_{app} indicates a large change in the mixture's order parameter S . In reality both individual order parameters S_i have close values in a homogenous mixture, and the assumption of their equality leads to eqn 3. Thus, knowing molecular parameters C_i , the mixture's order parameter S can be calculated. The relationship between S ,

Table 4 Bulk parameters for **2** calculated using the Maier–Meier equation^a

A				
	A	B	C	D
Computed values				
<i>In 6-CHBT solution</i>	$g = 0.47 \pm 0.04$	$g = 0.59 \pm 0.09$	$g = 0.67 \pm 0.05$	$g = 0.69 \pm 0.08$
ϵ_{\parallel}	1.1 ± 0.2	2.5 ± 0.5	4.2 ± 0.25	4.7 ± 0.5
ϵ_{\perp}	6.4 ± 0.2	6.8 ± 0.4	6.5 ± 0.25	6.8 ± 0.5
$\Delta\epsilon$	-5.4	-4.3	-2.3	-2.1
S_{app}	$6.3 (5.1-8.2)^b$	$2.2 (1.7-3.0)^b$	$0.70 (0.63-0.78)^b$	$0.69 (0.57-0.87)^b$
<i>In 6-CHBT solution</i>		For $S_{\text{app}} = 0.7, g = 1.0$		
ϵ_{\parallel}	5.4	5.3	4.7	5.3
ϵ_{\perp}	7.7	8.3	8.6	8.9
$\Delta\epsilon$	-2.4	-3.1	-3.9	-3.6
<i>Pure compound</i>		For $S = 0.7, g = 1.0$		
ϵ_{\parallel}	5.2	5.0	4.6	5.1
ϵ_{\perp}	7.4	7.7	8.2	8.5
$\Delta\epsilon$	-2.2	-2.7	-3.6	-3.4
ϵ_s	6.43	7.03	6.65	7.61

^a Computed using molecular parameters listed in Table 3 and experimental $\Delta\epsilon$ in Table 2. The ϵ_s is an isotropic static permittivity obtained by numerical solving the Debye equation using theoretical α and μ . It is used to calculate parameters F and h . For details see text and ESI.

^b Range of values which correspond to the uncertainty of the g parameter.

S_{app} , and order parameter of the pure host S_{host} is expressed by eqn 4.

$$\Delta\epsilon = C_1 S_1 x + C_2 S_2 (1 - x) \quad (2)$$

$$\Delta\epsilon = S [C_1 x + C_2 (1 - x)] \quad (3)$$

$$S = S_{\text{host}} + \frac{1}{1 + \alpha} (S_{\text{app}} - S_{\text{host}}) \quad (4)$$

where $\alpha = \frac{C_{\text{host}}(1-x)}{C \bullet x}$

The molecular parameter C_{host} for the host was calculated from $\Delta\epsilon$ and literature⁵⁰ order parameter $S_{\text{host}} = 0.67$ at 25 °C. Parameters C for the additives **2** were calculated according to the Maier–Meier equation and using the estimated Kirkwood parameter g (Table 4). It should be noted that the resulting parameters listed in Table 5 depend on the medium (F and h), g , and T , and also the Kirkwood parameter g depends on T and the medium (host). For simplicity, factors F and h were assumed to be the same in the range of the concentrations as for the pure host. Estimates show that these values are less than 1% different than those for the actual mixtures.

From parameters C_i for the mixture's components and experimental $\Delta\epsilon$ for the solutions, order parameter S was calculated for each concentration according to eqn 4, and the results are shown in Fig. 6.

Table 5 Molecular components of dielectric anisotropy^a

	6-CHBT	2A	2B	2C	2D
C	10.60	-0.84	-1.97	-3.30	-2.99

^a Calculated from experimental data for 6-CHBT and using eqn 1 for **2**. For details see text and ESI.

The data in Fig. 6 clearly show a large decrease of the mixture's order parameter S for solutions of carborane derivatives **2A** and **2B**. Thus, addition of about 15 mol% of either compound results in a decrease of S by nearly 10%! In contrast, the BCO and terphenyl derivatives **2C** and **2D** have practically no effect on the S parameter within the assumed modest error limits of $\pm 2\%$. It is interesting to note that the computed S values change monotonically with concentration for **2A** and **2C** for which the highest correlation of the dielectric data was observed (Table 2). Conversely, the observed scattering of datapoints for **2B** and **2D** reflects lower quality of dielectric data correlation for these compounds (*vide supra*).

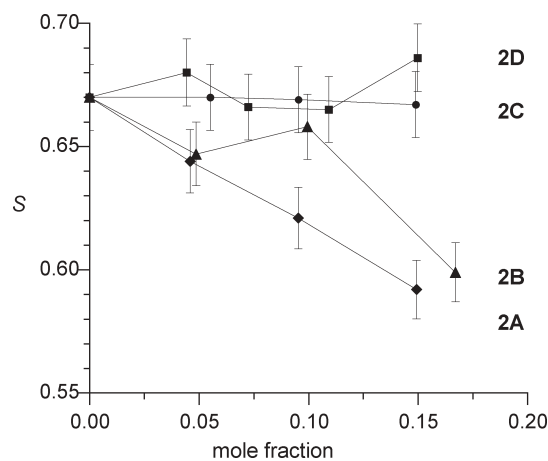


Fig. 6 Plot of order parameter S for 6-CHBT solutions vs. mole fraction of **2A** (◆), **2B** (▲), **2C** (●), and **2D** (■). Parameter S was calculated using eqn 4 and data in Table 5. The lines are guides for the eye. The error bar is set at 2%.

structure–property analysis. Further, dielectric parameters for the host and mixtures, and consequently the resulting extrapolated values depend also on the type of cell used, the orienting layer, the pretilt angle, and the definition of the threshold voltage V_{TH} (% of raise). Thus, for polyimide-coated cells used in this work with the pretilt of 2° – 3° , the values obtained for the host are lower than those reported in the literature. In contrast, preliminary experiments in SiO_2 -coated cells with practically 0.0 pretilt angle showed that although the measured permittivity values were higher, the trend in the extrapolated values for additives **2** remains the same. Thus, the observed trends are fully reproducible and suggest a strong correlation with molecular parameters (such as in Fig. 7), but the quantitative relationship between the structure and dielectric behaviour will require more detailed and precise experiments.

Results presented here contribute to a better understanding of the impact of carborane derivatives on materials properties and the formulation of mixtures in general. They also shed more light on the dielectric values that are typically extrapolated from 10%–20% solutions of either mesogenic or non-mesogenic compounds.^{2,7,8,55} For structurally similar compounds and very low concentrations, the impact of the additive on a material's order parameter is minimal. For higher concentrations and less sterically compatible components, such as carborane-containing compounds, the order parameter of the mixture may be affected strongly by the dopant. Consequently, dielectric and optical properties of such mixtures may exhibit strong non-linear behavior.

Finally, the use of a differently defined ring size requires a comment. Thus, correlation in Fig. 3 uses the effective ring diameter d_e , while the VDW diameter of the cylinder of ring rotation, d_c , is used for analysis of data in Fig. 7. It can be argued that effective ring size d_e is appropriate for correlation of clearing temperatures (such as in Fig. 3), since it is directly related to the packing fraction of the mesogen.⁵⁶ Steric effects exerted by a molecule on the environment and order parameter, may be correlated with the diameter of the rotating ring d_c . For rings **A**–**C** the two diameters d_e and d_c are the same, while for benzene the diameter of the cylinder of rotation d_c is 6.66 Å instead of the effective ring size $d_e = 5.03$ Å.

Conclusions and summary

Experimental results demonstrate that thermal and dielectric properties of pure compounds and binary mixtures depend on the steric factors of the compounds and scale with the ring size. Thus the depression of the clearing point upon lateral fluorination can be quantitatively correlated with the effective ring size. It is suggested that the slope of the linear fit provides a measure of the effectiveness of shielding of the substituent by ring **A** and is related to the number and position of the substituents relative to ring **A**. More experimental work involving other substituents and structural motifs is needed to establish the generality of this correlation.

Dielectric results for low concentration nematic solutions give information about host–additive interactions and their structural compatibility. The calculated apparent order

parameter S_{app} reflects the effect of the dopant on the order parameter of the mixture. Thus, a large apparent order parameter S_{app} required by the theory for the extrapolated dielectric values for **2** implies a large decrease of the actual order parameter S of the solution in 6-CHBT. In series **2** the S_{app} increases with the increasing size of the ring **A**; the larger the ring the higher steric demands of the additive, the higher apparent order parameter S_{app} , and the lower actual order parameter S of the solution.

Experiment and theory are consistent and show that an increase in the size of ring **A** (and hence decrease in order parameter) strongly affects the ϵ_{\parallel} but weakly affects ϵ_{\perp} of a host with $\Delta\epsilon > 0$. In consequence, the addition of a sterically demanding dopant such as **2A** with $\Delta\epsilon < 0$ excessively lowers the ϵ_{\parallel} component, which results in lower $\Delta\epsilon$ values as compared to more sterically compatible dopants such as **2C**. Further studies are needed to provide higher quality dielectric data and quantitative correlations, and also to understand how additives **2** affect dielectric properties of a host with $\Delta\epsilon < 0$ and whether similar excessive increase of the negative $\Delta\epsilon$ values can be observed upon addition of **2A** and **2B**.

The protocol used in this work to analyze dielectric results for binary mixtures consists of three steps. First, using extrapolated $\Delta\epsilon$, computed molecular values, and field parameters for the pure host, Kirkwood parameter g is fitted to calculate back the extrapolated values ϵ_{\parallel} and ϵ_{\perp} . This procedure also gives the S_{app} . Secondly, using the resulting g value, the molecular constant C is calculated for the additive from the Maier–Meier equation. Finally, the order parameter of the mixtures is computed from the additivity of $\Delta\epsilon$.

Experimental

Optical microscopy and phase identification were performed using a PZO “Biolar” polarized microscope equipped with a HCS250 Instec hot stage. Thermal analysis was obtained using a TA Instruments 2920 DSC. Transition temperatures (onset) and enthalpies were obtained using small samples (1–2 mg) and a heating rate of $5^{\circ}\text{C min}^{-1}$ under a flow of nitrogen gas. The clearing transition was typically less than 0.3°C wide.

E-4-(4-Hexylcyclohexyl)phenyl isothiocyanate (6-CHBT) was purified by vacuum distillation before use. The measurements for the pure host at 23°C : $V_{\text{TH}} = 1.73 \pm 0.02$ V; $\epsilon_{\parallel} = 11.0 \pm 0.1$; $\epsilon_{\perp} = 3.9 \pm 0.1$; $\Delta\epsilon = 7.1 \pm 0.1$; Literature values:⁵⁷ $V_{\text{TH}} = 1.63$; $\epsilon_{\parallel} = 12.0$; $\epsilon_{\perp} = 4.0$; $\Delta\epsilon = 8.0$.

Dielectric measurements

Properties of compounds in series **2** were measured by a Liquid Crystal Analytical System (LCAS - Series I, LC Analytical Inc.) using GLCAS software version 0.59 which implements literature procedures for dielectric constants.⁵⁸

Approximately 5, 10 and 15 mol% solutions of **2** in 6-CHBT were prepared and conditioned for 24 h at 50°C . Thermal analysis of each mixture (DSC) showed linear dependence of both onset and peak temperature of the transition on mole fraction x . The onset transition temperatures were fitted to $T_{\text{NI}} = 42.0 + xT_{\text{onset}}$ and gave the extrapolated values which are higher by $+12^{\circ}\text{C}$, -2°C , $+28^{\circ}\text{C}$, $+6^{\circ}\text{C}$ than those for pure **2A**–**2D**, respectively ($r^2 > 994$, error $< \pm 2.5^{\circ}\text{C}$).

The mixtures were loaded into ITO electro-optical cells by capillary forces at ambient temperature. The cells (about 5 μm thick, electrode area of 0.28 cm^2 and antiparallel rubbed polyimide layer 2°–3° pretilt) were obtained from LCA Inc. and their precise thickness ($\pm 0.05 \mu\text{m}$) was measured by optical methods. The filled cells were heated to an isotropic phase and were left for an hour at room temperature before measurement.

Default parameters were used for measuring dielectric constants of the mixtures: triangular shaped voltage bias ranging from 0.1–20 V at 1 kHz frequency. The threshold voltage V_{th} was measured as a 10% of change. For each mixture the measurement was repeated at least ten times. The first two results were rejected and the rest of consistent results were averaged to calculate the mixture's parameters. Values for dielectric permittivity ϵ were plotted as a function of concentration and extrapolated to pure **2**. The intercept in the fitting functions was fixed at the value for the pure host. The results are presented in Table 2 and details are listed in ESI†.

Suzuki coupling of halides **7** and boronic acid **8**. General procedure for the preparation of **1–6**

Method A¹⁸. A mixture Pd(PPh₃)₄ (0.03 mmol), toluene (5.0 mL), aryl halide **7** (1.0 mmol), and an aqueous solution of Na₂CO₃ (1.0 mL of a 2 M solution) under nitrogen atmosphere, and then boronic acid **8** (1.1 mmol) in EtOH (1.0 mL) was added. The mixture was refluxed at a temperature of 110 °C for approximately 24 h under vigorous stirring and the progress monitored by TLC analysis (hexane: CH₂Cl₂, 9 : 1). The reaction mixture was poured into water, the product was extracted with CH₂Cl₂, extracts washed with brine, and dried (Na₂SO₄). The solution was passed through a silica gel plug, solvent was evaporated and the resulting solid was purified chromatographically on silica gel.

Final purification for analysis was performed as follows: each compound was dissolved in CH₂Cl₂, solution filtered through cotton to remove particles, evaporated and the product recrystallized from the indicated solvent until constant temperature. The resulting crystals were dried in vacuum overnight at ambient temperature. The purity was confirmed by combustion analysis. All analytical data (NMR, combustion analysis and MS) are provided in ESI†.

Method B. Boronic acid **8** (0.17 mmol), aryl halide **7** (0.14 mmol), and Pd(AcO)₂ (1.0 mg) were dissolved in degassed *N*-methylpyrrolidinone (NMP, 1.5 mL). The flask was flushed with argon and heated to 50 °C. Tricyclohexylphosphine (2.0 mg) was added, and the mixture was stirred for 10 min. A 2.5 M solution of K₃PO₄ (1.0 mL) was added and the reaction was stirred at 90 °C for 8 h under Ar. The reaction mixture was poured onto water, and the product was extracted into EtOAc. The organic extract was washed with brine and dried (Na₂SO₄). Further purification as described in Method A.

Acknowledgements

This project was supported by the NSF grant (DMR-0111657). We thank Dr Serhii Pakhomov for his help with the

preparation of **6A**, Mr Po-Chih Chen for technical assistance, and Ms Krystyna Kulikiewicz for help with obtaining several NMR spectra. We are also grateful to Dr Eike Poetsch of E. Merck for the gift of 4-bromo-4'-pentylbiphenyl (**7D**).

References

- 1 P. Kirsch and M. Bremer, *Angew. Chem., Int. Ed.*, 2000, **39**, 4216–4235.
- 2 D. Pauluth and K. Tarumi, *J. Mater. Chem.*, 2004, **14**, 1219–1227.
- 3 V. Reiffenrath, J. Krause, H. J. Plach and G. Weber, *Liq. Cryst.*, 1989, **5**, 159–170.
- 4 G. W. Gray, M. Hird, D. Lacey and K. J. Toyne, *J. Chem. Soc., Perkin Trans. 2*, 1989, 2041–2053.
- 5 P. Kirsch, V. Reiffenrath and M. Bremer, *Synlett*, 1999, 389–396.
- 6 M. Bremer and L. Lietzau, *New J. Chem.*, 2005, **29**, 72–74.
- 7 M. Klasen, M. Bremer and K. Tarumi, *Jpn. J. Appl. Phys.*, 2000, **39**, L1180–L1182.
- 8 G.-X. Sun, B. Chen, H. Tang and S.-Y. Xu, *J. Mater. Chem.*, 2003, **13**, 742–748.
- 9 C. C. Dong, P. Styring, J. W. Goodby and L. K. M. Chan, *J. Mater. Chem.*, 1999, **9**, 1669–1677.
- 10 V. Vill, *Liq Cryst 4.3*, ed. N. Harris, H. Sajus and G. Peters, 2002, LCI Publisher GmbH, Hamburg, Germany, database and references therein.
- 11 K. J. Toyne, in *Thermotropic Liquid Crystals*, ed. G. W. Gray, Wiley, New York, 1987, pp. 28–63.
- 12 A. Januszko, P. Kaszynski, M. D. Wand, K. M. More, S. Pakhomov and M. O'Neill, *J. Mater. Chem.*, 2004, **14**, 1544–1553.
- 13 W. Piecek, J. M. Kaufman and P. Kaszynski, *Liq. Cryst.*, 2003, **30**, 39–48.
- 14 P. Kaszynski and A. G. Douglass, *J. Organomet. Chem.*, 1999, **581**, 28–38.
- 15 A. Januszko, P. Kaszynski, K. Ohta, T. Nagamine, V. G. Young, Jr. and Y. Endo, in preparation.
- 16 A. Januszko, P. Kaszynski and W. Drzewinski, *J. Mater. Chem.*, 2006, **16**, 452–461.
- 17 B. Ringstrand, J. Vroman, D. Jensen, A. Januszko, P. Kaszynski, J. Dziaduszek and W. Drzewinski, *Liq. Cryst.*, 2005, **32**, 1061–1070.
- 18 N. Miyaura, Y. Yanagi and A. Suzuki, *Synth. Commun.*, 1981, **11**, 513–519.
- 19 Pure carborane derivatives with sharp transition temperatures can be obtained only after repeated recrystallization, but 10-vertex derivatives in general do not crystallize well.
- 20 K. Czuprynski, A. G. Douglass, P. Kaszynski and W. Drzewinski, *Liq. Cryst.*, 1999, **26**, 261–269.
- 21 H. O. Wirth, O. Königstein and W. Kern, *Liebigs Ann. Chem.*, 1960, **634**, 84–104.
- 22 G. W. Gray and S. M. Kelly, *J. Chem. Soc., Perkin Trans. 2*, 1981, 26–31.
- 23 A. G. Douglass, S. Pakhomov, B. Reeves, Z. Janousek and P. Kaszynski, *J. Org. Chem.*, 2000, **65**, 1434–1441.
- 24 Z. Janousek and P. Kaszynski, *Polyhedron*, 1999, **18**, 3517–3526.
- 25 S. Sharma, D. Lacey and P. Wilson, *Liq. Cryst.*, 2003, **30**, 451–461.
- 26 M. R. Friedman, K. J. Toyne, J. W. Goodby and M. Hird, *Liq. Cryst.*, 2001, **28**, 901–912.
- 27 M. C. Artal, K. J. Toyne, J. W. Goodby, J. Barberá and D. J. Photinos, *J. Mater. Chem.*, 2001, **11**, 2801–2807.
- 28 H. Dorn, J. M. Rodenzo, B. Brunnhöfer, E. Rivard, J. A. Massey and I. Manners, *Macromolecules*, 2003, **36**, 291–297.
- 29 I. Dierking, *Textures of Liquid Crystals*, Wiley-VCH, Weinheim, 2003.
- 30 G. W. Gray and J. W. G. Goodby, *Smectic Liquid Crystals-Textures and Structures*, Leonard Hill, Philadelphia, 1984.
- 31 D. Demus and L. Richter, *Textures of Liquid Crystals*, 2nd edition, VEB, Leipzig, 1980.
- 32 G. W. Gray, M. Hird and K. J. Toyne, *Mol. Cryst. Liq. Cryst.*, 1991, **195**, 221–237.
- 33 The geometrical parameters for each ring were calculated (HF/6-31G(d)) and corrected for H and C (benzene) van der Waals radii (1.2 Å and 1.7 Å respectively). Benzene was treated as an ellipsoid and the diameter d represents an average of the two axes a and b :

- A: $d = 7.43 \text{ \AA}$; B: $d = 7.17 \text{ \AA}$; C: $d = 6.72 \text{ \AA}$; D: $d = 5.03 \text{ \AA}$
($a = 6.66 \text{ \AA}$, $b = 3.40 \text{ \AA}$).
- 34 T. Nagamine, A. Januszko, K. Ohta, P. Kaszynski and Y. Endo, *Liq. Cryst.*, 2005, **32**, 985–995.
- 35 A. G. Douglass, K. Czuprynski, M. Mierzwa and P. Kaszynski, *J. Mater. Chem.*, 1998, **8**, 2391–2398.
- 36 K. Czuprynski and P. Kaszynski, *Liq. Cryst.*, 1999, **26**, 775–778.
- 37 Details including method selection are given in the ESI†.
- 38 C. Hansch, A. Leo and R. W. Taft, *Chem. Rev.*, 1991, **91**, 165–195 and references therein.
- 39 L. I. Zakharkin, V. N. Kalinin and E. G. Rys, *Bull. Acad. Sci. USSR, Div. Chem. Sci.*, 1974, 2543–2545.
- 40 The σ_p value for adamantane was used instead: H. Alper, E. C. H. Keung and R. A. Partis, *J. Org. Chem.*, 1971, **36**, 1352–1355.
- 41 M. Charton, *Prog. Phys. Org. Chem.*, 1981, **13**, 119–251.
- 42 P. Kaszynski, S. Pakhomov, K. F. Tesh and V. G. Young, Jr., *Inorg. Chem.*, 2001, **40**, 6622–6631.
- 43 W. Maier and G. Meier, *Z. Naturforsch.*, 1961, **16A**, 262–267 and 470–477.
- 44 S. Urban, in *Physical Properties of Liquid Crystals*, ed. D. Nematics, A. Dunmur, Fukuda, and G. Luckhurst, IEE, London, 2001, pp. 267–276.
- 45 Z. Raszewski, R. Dabrowski, Z. Stolarzowa and J. Zmija, *Cryst. Res. Technol.*, 1987, **22**, 835–844.
- 46 P. Bordewijk, *Physica*, 1974, **75**, 146–156.
- 47 P. Kedziora and J. Jadzyn, *Acta Phys. Pol.*, 1990, **A77**, 605–610.
- 48 G. Saitoh, M. Satoh and E. Hasegawa, *Mol. Cryst. Liq. Cryst. Sci. Technol., Sect. A*, 1998, **301**, 13–18.
- 49 M. Klasen, M. Bremer, A. Götz, A. Manabe, S. Naemura and K. Tarumi, *Jpn. J. Appl. Phys.*, 1998, **37**, L945–L948.
- 50 S. Urban, J. Kedzierski and R. Dabrowski, *Z. Naturforsch.*, 2000, **55A**, 449–456.
- 51 K. Ohta, A. Januszko, P. Kaszynski, T. Nagamine, G. Sasnouski and Y. Endo, *Liq. Cryst.*, 2004, **31**, 671–682.
- 52 For example see: D. Demus, in *Handbook of Liquid Crystals*, ed. D. Demus, J. Goodby, G. W. Gray, H.-W. Spiess, and V. Vill, Wiley-VCH, 1998, vol. 1, pp. 151–153. Also ref. 10 and citation therein.
- 53 Based on eqn 4, a reverse relationship between S and S_{app} is expected when both dopant and the host have the same sign of dielectric anisotropy or $|\Delta\epsilon(\text{host})| < |\Delta\epsilon(\text{dopant})|$.
- 54 Z. Raszewski, *Liq. Cryst.*, 1988, **3**, 307–322.
- 55 S. Naemura, in *Physical Properties of Liquid Crystals: Nematics*, ed. D. Dunmur, A. Fukuda, and G. Luckhurst, IEE, London, 2001, pp. 523–581.
- 56 D. Demus and A. Hauser, in *Selected Topics In Liquid Crystal Research*, ed. H. D. Koswig, Akademie-Verlag, Berlin, 1990, pp. 19–44.
- 57 R. Dabrowski, *Mol. Cryst. Liq. Cryst.*, 1990, **191**, 17–27.
- 58 S.-T. Wu, D. Coates and E. Bartmann, *Liq. Cryst.*, 1991, **10**, 635–646.